

HOW GOOD ARE HARTREE-FOCK CHARGE DENSITIES ?

X. CAMPI

(Communication to the IAEA Conference on "Hartree-Fock and self-consistent field theories in nuclei" - Trieste 24.2 to 1.3. 1975)

IPNO/TH 75-14

- February 1975 -

FR502210

HOW GOOD ARE HARTREE-FOCK CHARGE DENSITIES ?

X. CAMPI

Division de Physique Théorique², Institut de Physique Nucléaire
91406 - ORSAY - France

Abstract : The principle characteristics of Hartree-Fock charge densities (mean square radius, surface thickness, quantum fluctuations) calculated using different effective interactions are discussed in terms of their nuclear matter properties (Fermi momentum, effective mass, incompressibility). A comparison with the experimental charge distributions is made. Differences between the charge densities of neighbouring nuclei (isotope and isotone shifts) are also considered and the main factors governing these effects are discussed.

1. Introduction

An overall description of those nuclear properties which depend essentially on the average field has been obtained in recent years in the framework of the self-consistent methods, generally called Hartree-Fock methods. Among these nuclear properties the charge density ρ_{ch} appears to be the richest source of information by which the validity of these methods can be studied. The principle aim of this work is to examine how well the calculated densities agree with experiment but more important, from this comparison and from the comparison of results of different methods, to determine what are the theoretical ingredients which determine the principal characteristics of the density.

Our attention will be concentrated mainly on proton-neutron nuclei, for which a Hartree-Fock description can be justified. We will discuss only those theories which give a correct saturation in infinite nuclear matter, this being an indispensable condition for obtaining realistic charge densities. All of these theories are more or less based on the Brueckner theory and upon the local density approximation (LDA). They all contain a certain amount of phenomenology which is relatively small in the theories

called Density Dependent Hartree-Fock (DDHF), and rather greater for those which use purely phenomenological effective forces of the Skyrme or Moszkowski type. We will attempt to demonstrate how these ingredients, which are poorly defined from a theoretical point of view, influence the calculated densities.

In the section 2 we will compare the results of different calculations with experiment and in section 3 we will attempt to interpret these results. Section 4 is devoted to the somewhat different problem of differences in the charge density between neighbouring nuclei (isotope and isotone shift).

2. Comparison of Hartree-Fock charge densities with experiment

The best test of the quality of Hartree-Fock charge densities is the direct comparison with experiment of the calculated electron scattering cross sections $d\sigma/d\Omega$ and muonic atoms transition energies E_n . This is because the theories for electron scattering and for the energy levels of muonic atoms are among the best established theories in nuclear physics and there are reasons to believe that the quantum electrodynamics corrections which we are not yet able to calculate properly, will change the present results very little. At the same time, it should be pointed out that in this direct comparison it is difficult to recognize the origin of particular disagreements or even of accidental agreements between experiment and theory.

To understand the origin of the short-comings of the various theories it is more instructive to discuss the behaviour of ρ_{ch} in real space. This indirect comparison was for a long time discredited by the fact that the so-called experimental ρ_{ch} were very model dependent, being simply a Fermi or other function containing two or three parameters fitted to experiment. More recently, other methods of greater reliability have been introduced which greatly reduce the model dependence of these experimental ρ_{ch} . In the method of Friar and Negle¹⁾, one divides the charge density into two parts. The first, ρ_0 , could be a Fermi function or a calculated Hartree-Fock charge density. To this is added a correction ρ_1 which is expressed as a finite sum Fourier series

² Laboratoire associé au C.N.R.S.

based on an interval $0.4r$ fm. The outer radius of this density correction is chosen at the outer edge of the charge density, where the density is small and in fact the error in its determination becomes comparable with ρ . The number of coefficients which can be determined in ρ_1 is a function of the range of momentum transfer covered by the experimental data. The coefficients are chosen so as to give the smallest mean square error between the experimental data and the calculated cross sections and muonic X-rays. The fitting procedure determines both the coefficients and their mean square error. These errors can be transformed into real space and provide an error envelope for the fitted charge density. This error envelope gives an idea of the range of ρ_{ch} which would be compatible with the given experimental data. Except very close to $r = 0$, this error envelope (representing the effect of the experimental errors), is greater than a reasonable estimate of the error due to the truncation of the series expansion of ρ_1 . An alternative method due to Sick²⁾ expresses ρ as a sum of Gaussian distributions each one centered at a different radial distance from the origin. Various conditions are imposed to ensure that the minimum wavelength of any oscillation in the density exceeds 1 fermi. By making a number of fits to the experimental data sick is also able to produce an error envelope for the charge density.

In Fig. 1 are shown the experimental ρ_{ch} which are available at the present time. Those for ^{40}Ca and ^{44}Ca are from the analysis by Sick²⁾ using his method. He finds that with the current experimental data there is an ambiguity in the determination of the central density of ^{40}Ca ; one of these densities is very flat and the other has a peak at the origin but both give practically the same χ^2 for electron scattering. The ρ_{ch} of ^{208}Pb was determined by Friar and Negele using five different electron scattering experiments and six pieces of muonic atom data. This is the case for which both the data and the analysis are most complete. For ^{82}Zr the analysis was carried out using the Friar-Negele method by Sprung³⁾ using the electron scattering data of ref. 5) at 300 MeV ($q_{max} = 2.79 \text{ fm}^{-1}$) and the muonic atom transition data from the compilation by Engler et al.⁶⁾. The ρ_{ch} of ^{58}Ni , a good proton closed shell nuclei, was obtained by Sick using the very high momentum transfer data ($q \approx 4 \text{ fm}^{-1}$) recently measured by the Saclay group⁷⁾.

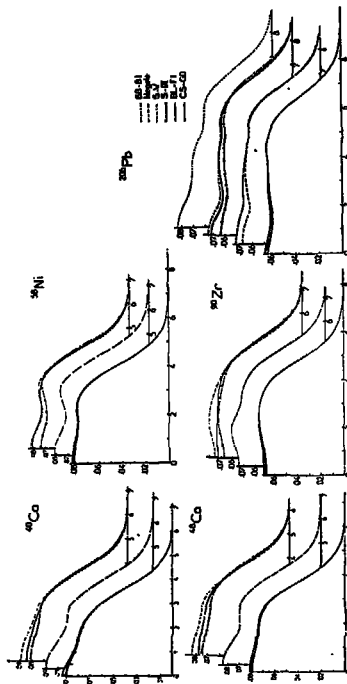


Fig. 1 - Charge density distributions. Theoretical densities: 1) Friar-Negele ref. 4), 2) Friar-Negele ref. 5), 3) Sprung ref. 3), 4) Engler et al. ref. 6), 5) Sick ref. 2), 6) Friar-Negele ref. 4), 7) Friar-Negele ref. 4), 8) Friar-Negele ref. 4), 9) Friar-Negele ref. 4), 10) Friar-Negele ref. 4), 11) Friar-Negele ref. 4), 12) Friar-Negele ref. 4), 13) Friar-Negele ref. 4), 14) Friar-Negele ref. 4), 15) Friar-Negele ref. 4), 16) Friar-Negele ref. 4), 17) Friar-Negele ref. 4), 18) Friar-Negele ref. 4), 19) Friar-Negele ref. 4), 20) Friar-Negele ref. 4).

In Fig. 1 we also show for comparison the charge densities calculated in Hartree-Fock. In the following sections we will attempt to interpret the differences between experiment and these calculations on the one hand and between different calculations themselves on the other hand.

3. Interpretation and principle characteristics of Hartree-Fock densities

The big advantage in looking at ρ_{ch} instead of $F(\rho)$ is that one can use more physical intuition in attempting to recognize the origin of certain salient features of the density, such as the average interior density, the amplitude of the Friedel oscillations and the surface thickness. This analysis, however, remains qualitative, partly because it is difficult to give an exact definition of these characteristics and partly because it is difficult to say precisely which aspects of the theory really determine a particular characteristic of the density.

Because the theoretical situation is rather clearer in the case of infinite nuclear matter than in finite nuclei, what we will do, and what is generally done, is to attempt to explain the differences in the charge density between different theories in terms of the differences found in nuclear matter for such quantities such as saturation, k_F , the binding energy per particle E/A , the incompressibility K , the symmetry energy E_{sym} and the effective mass m^* . The criticism of this approach is that these five quantities do not completely characterize any given theoretical framework nor even properties of a given interaction within such a framework. These comparisons will have more sense for heavy nuclei where the connection with nuclear matter is more valid and the validity of the local density approximation more likely. Friar and Negele⁸⁾ have carried out such a comparison between different calculations in a very careful and complete manner for the density of ²⁰⁸Pb. Many of their conclusions will be reflected in the following discussion.

3.1 Relation between k_F , E/A_{NM} and the Mean Square Radius

The radial moments are among the few characteristic of the density which are objectively well defined. There

is no exact relation between k_F and the mean square radius r but from simple arguments, for example the liquid drop model (neglecting surface tension and Coulomb effects), one expects that r will depend strongly on k_F . We have in this case a relation

$$Ar = - \sqrt{\frac{2}{3}} \left[\frac{2\pi h}{k_F} \right]^{1/3} \frac{1}{k_F} Ar_F \quad (1)$$

A more precise relation can be obtained numerically by varying slightly the saturation density of a realistic effective interaction, as one does phenomenologically to take account of higher order corrections. Thus, for example, readjusting the effective force of Sprung and Banerjee⁹⁾ we have found the following relationship which are valid in the neighbourhood of $k_F = 1.35 \text{ fm}^{-1}$ and $E/A_{NM} = 16.5 \text{ MeV}$:

$$Ar_{10} = - 0.03 \Delta(E/A)_{NM} - 0.65 \Delta k_F \quad (1^{10})$$

$$Ar_{20} = - 0.04 \Delta(E/A)_{NM} - 3.0 \Delta k_F \quad (2^{10})$$

A similar behaviour is seen¹⁰⁾ for different Skyrme forces which saturate nuclear matter in the range $k_F = 1.29$ (S-III) to $k_F = 1.32$ (S-V). In any case it is seen that the dependence of r on k_F is quite strong and it is well to remember that k_F has no well defined theoretical value. The Reid soft core force used in most of the calculations of the realistic effective interactions gives a nuclear matter value $k_F = 1.44 \text{ fm}^{-1}$. No realistic force gives saturation at a lower Fermi momentum. At the present time to obtain reasonable r.m.s. radii one must adjust k_F phenomenologically.

The relation 2 also indicates the dependence of r_{20} on the binding energy per particle $(E/A)_{NM}$ of nuclear matter according to the calculations of ref. 11). This quantity $(E/A)_{NM}$ must also be adjusted phenomenologically in order to obtain the correct binding energy of finite nuclei. The dependence of r_{20} on $(E/A)_{NM}$ is not negligible, taking into account that its theoretical value is not known to better than 1 MeV per particle from the semi-empirical mass formula or from H.F. calculations.

Although the absolute value of r_{20} for a given nucleus is not well defined by the theory, its variation with the mass number A should be, at least for the medium and heavy nuclei to which the present theories are applicable. This is because the

variation of the radius depends critically on a balance between the volume, surface and Coulomb energy parts of the mean nuclear field. It is this balance which one hopes to have correctly reproduced by using a realistic nuclear force in the Brueckner theory. We will examine this variation of the charge radius with A for a number of different calculations. In Fig.2 is shown the percentage deviation $(100 \cdot (r_C^{th} - r_C^{exp}) / r_C^{exp})$ for the five standard doubly-magic nuclei. Grouped in Fig.2a) are the calculations based on purely phenomenological forces. These include the force of Ehlers and Moszkowski¹²⁾ called the MDI force, the Skyrme forces S-III and S-V of Belner et al¹⁰⁾, that of Belner and Losbard¹³⁾ called force BL-FI. In Fig.2b) are shown the results for the realistic effective interactions of Fai and Nenech¹⁴⁾ denoted FN-S, Coon and Kohler¹⁵⁾ denoted CK, and the force C-0 of Campi and Sprung¹¹⁾ denoted CS.

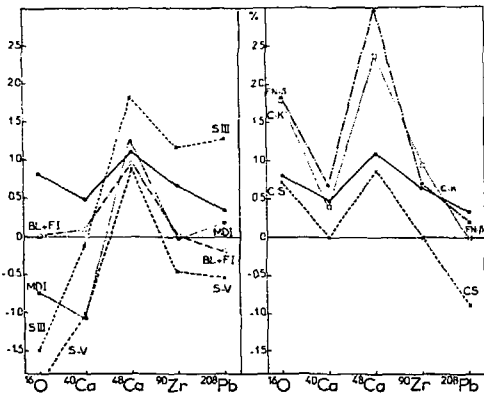


Fig.2

The continuous line in Fig.2 shows the contribution from the neutron form factor and from the electromagnetic spin orbit interaction¹⁶⁾. This correction can be taken into account by reading the quoted deviations with respect to this continuous line. A slight adjustment in the nuclear matter K_0 for any one of these forces could greatly improve the agreement with experiment while including these corrections.

The main impression which one obtains from Fig.2 is that by including the neutron and electromagnetic spin orbit corrections to the form factor the behaviour of the radii against A is very good for most of the calculations. The simultaneous agreement of binding energies and radii is a significant achievement of the Hartree-Fock-LDA theories. In particular it is reassuring to note that the quality of agreement is practically as good for the realistic effective forces as for the purely phenomenological ones, where the parameters were adjusted in order to obtain this agreement.

Leaving aside ^{16}O for which the effects of the center of mass motion are too large, the principle discrepancy observed is for the case of ^{46}Ca . This is particularly visible for the forces MDI, S-III, S-V, C-K and FN-S. We will discuss the question of the ^{44}Ca - ^{46}Ca isotope shift in more detail in Section 4.

3.2 Surface Thickness and Quantum Density Fluctuations.

Relation to m^2 , K , and Density Dependence

A second characteristic quantity for the charge density which can be defined without great ambiguity is the surface thickness. For a heavy nuclei one can define an average central density. The slope of ρ at the half density point provides a natural definition of surface thickness. This was done for example by Friar and Negele⁸⁾ in their analysis of Hartree-Fock calculations for Pb. For lighter nuclei it becomes difficult to define a half density radius and therefore a different definition of surface thickness is required. One possibility which gives an average over the entire surface region is suggested by the behaviour of the radial moments

$$R_k = \left[\frac{k+3}{3} r_p k. \right]^{1/k}$$

For a Fermi-like distribution one has

$$\rho = \rho_0 \left[1 + \exp\left(\frac{\epsilon - \mu}{kT}\right) \right]^{-1}$$

$$R_k = R \left[1 + \frac{r_p^2}{b^2} (k+5) \left(\frac{\rho}{R} \right)^2 + \dots \right]$$

The slope $\frac{dR_k}{dk} = -\frac{r_p^2}{b^2} \frac{\rho^2}{R^2}$ (3) contains information about the surface thickness. This is the definition of "surface thickness" which we will adopt in the following.

As has been emphasized in the work of ref.8) the surface thickness is governed essentially by the range of the nuclear interaction and this occurs in two ways: through the direct and exchange Hartree-Fock potentials. The Hartree potential can be expressed as a convolution of the interaction with the density. The greater the range of the nuclear force, the more diffuse the local Hartree potential will become and the more diffuse the density will be. On the other hand, the non-locality of the exchange potential increases with the range of the two-body force. In particular, for a contact interaction, the exchange potential is local. In terms of its equivalent local potential method¹⁷⁾ a greater non-locality implies a greater state dependence of the exchange field. This leads to a decreased density of s.n. states and the s.p. wave functions become out of phase in the surface region, which leads to a more diffuse surface.

Nogele and Friar⁸⁾ discuss the same effect in terms of the Perey mechanism. The scattering wave functions inside a non-local potential are suppressed in comparison to those of a local potential having the same phase shifts. For normalized wave functions the suppression inside the potential is compensated by an enhancement of the tail which also increases the surface thickness. This effect was studied quantitatively by Nogele¹⁸⁾.

For a Skyrme type force it is difficult to speak of the force range, but the same reasoning can be applied to the effective mass m^* which also measures the non-locality of the Hartree-Fock field. From Table 1 one sees for different nuclei and different forces a clear correlation between m^* and

the surface thickness calculated as $(dR_k/dk)_{k=2}$.

FORCE	NUCLEAR MATTER		SURFACE THICKNESS $(R'_k)_{k=2}$				
	m^*/m	K	^{40}Ca	^{60}Ca	^{116}Ni	^{208}Zr	^{238}Pu
S-VI	.95	364.	.091	.076	.071	.073	.046
S-III	.76	356.	.093	.080	.073	.077	.050
S-V	.38	306.	.100	.093	.082	.092	.064
BL-VI	.90	280.	.102	.086	.081	.079	.057
BB-31	-	190.	.103	.087	.088	.094	.086
CS-GO	-	190.	.103	.086	.081	.087	.066
Exp.	-	-	.104	.087	.085	.081	.060
$(R'_k)_{k=2}$ (ref.15)	-	-	-.003	-.006	-.003	-.004	-.004

TABLE 1

The strength of the density dependent force is also important. It gives rise to a repulsive field of a range smaller than that of the density independent part of the force. This affects the deep lying levels more than the weakly bound ones, compressing the entire spectrum and thus tending to localize the total Hartree-Fock field. This effect is easier to see for Skyrme forces, for which the rearrangement field has the simple form

$$V_{n,p}^{\text{red}}(r) = \frac{c_3}{4} (\rho^2(r) - \rho_{n,p}^2(r)) \quad (4)$$

One observes that a larger c_3 compresses the spectrum and decreases the surface thickness. For the forces with finite range density dependence it is more difficult to define a strength for the density dependent part but it is clear that the role played is equally important and can be seen in the compression of the spectrum of single particle states. Thus, for example, the force B1 of Brink and Boeker¹⁹⁾ which has a range of only 1.4fm but which is density independent, has in ^{238}Pu a surface thickness of .086, greater than any of the forces in Table 1.

Another point concerns the influence of the incompressibility K in nuclear matter. One should expect the

surface thickness to decrease as K increases and to tend towards a sharp surface as $K \rightarrow \infty$. This dependence is difficult to study, for it is difficult to vary K while keeping the other properties, in particular n^0 , constant. This is particularly clear for a Skyrme type force for which a relation

$$\frac{\hbar^2}{2m} = \frac{\hbar^2}{2m} - \frac{1}{k_F} - 15 \left(\frac{E}{\hbar^2} \right)_{\text{SH}} - \left(\frac{E}{\hbar^2} \right) K + 2 \tau_F \quad (4)$$

can be established²⁰). This explains in particular why it is not possible to vary the compressibility K very much for Skyrme forces while preserving reasonable values for E/A , k_F and n^0 ($0.5 < n^0 < 1$). Greater variation in K may be obtained, however, by changing the form of the density dependence, for example taking $\tau_{12}^0 = \alpha \cdot 1$, as done by Lessey²¹) or taking a more sophisticated form

$$\tau_{12}^0 = \alpha + \gamma z$$

as in the force MD14 of Faessler, Galonska, Gneke and Moszkowski²²) leading to $n^0/m = 0.49$ and $K = 200$ MeV. The density dependence of the three realistic effective forces G0, G1 and G2 of Sprang and Banerjee calculated from the Reid potential used a finite range force with respectively $\alpha = 1/4$, $1/3$ and 1 leading to $K = 180$, 210 and 300 MeV. Finite nuclei calculations with these three forces show that the surface thickness decreases as the compressibility increases¹¹).

In Table 1, we have also indicated the values of $(dn_x/dx)_{x=2}$ calculated from model independent experimental charge densities. Because the surface region is very well determined in these analysis one can take these values as experimental numbers for the surface thickness. From the comparison with experiment in Table 1, it is seen that the Skyrme interactions S-VI and S-III with large values of both n^0 and K should be rejected.

A final remark concerns the impact on the surface thickness of the corrections from the reference¹⁶), which are included in the quoted values of $(n^0)_{k=2}$ in Table 1. It is easy to see that the neutron contribution tends to make the surface sharper because the neutron charge distribution is positive at its center and negative outside. Hence at the surface of the nucleus there will be a tail of negative charge introduced. If we suppose

that the neutron form factor is of short range compared to nuclear dimensions one can make an expansion giving for the charge density due to the electromagnetic structure of the neutron²³),

$$\rho_c^n(r) = \frac{1}{8} \rho_n^0(r) \langle r_{1N}^2 \rangle + \frac{1}{120} \rho_n^{IV}(r) \langle r_{1N}^4 \rangle + \dots$$

where the mean square radius of the charge distribution of the neutron is about $\sim 0.12 \text{ fm}^2$. The leading term is by far the largest and shows that ρ_c^n will have a positive region at the shoulder of the density followed by a negative region in the tail thereby reducing the surface thickness. The importance of this effect is also shown in Table 1 (ΔR^*).

The nuclear surface about which we have been talking is in fact a particular case of a quantum density fluctuation. Although for these fluctuations it is somewhat difficult to give a measure, we have performed the following tentative analysis: From the origin up to the shoulder of the density one can determine the best straight line passing through the shoulder in the x^2 sense. We think that in all practical cases the shoulder can be identified without major ambiguities. Let $x_{\text{th}}^2(x_{\text{exp}}^2)$ be the so obtained value of x^2 when $\delta_{\text{th}}^2(x_{\text{exp}}^2)$ is used; they measure the interior density fluctuations.

In Table 2 we give the fluctuation ratio $v_{\text{th}}^2/x_{\text{exp}}^2$ for several nuclei and interactions. We see in Table 2 a large dispersion in the results and notice in particular that Skyrme-like interactions give smaller oscillations in the light nuclei than the long range interactions B1 and G-0, but the situation for ²⁴²Pb is the opposite.

To explain this particular effect Friar and Negele⁸), use an argument based on the relation between Hartree-Fock for a finite range force and Hartree-Fock using the DME²⁴). Considering the direct or Hartree potential one sees that for a finite range force the convolution with the density gives a potential where the density oscillations are washed out and that the density calculated self consistently in such a potential will have smaller oscillations typical of the smooth potential. On the other hand,

FGRC	Ratio of interior density fluctuations ρ_n/ρ_p exp				
	^{40}Ca	^{48}Ca	^{90}Zr	^{138}Xe	^{208}Pb
S-VI	1.2	0.1	0.4	1.3	1.1
S-III	1.0	0.2	0.7	1.8	1.2
S-V	2.0	1.4	1.6	3.7	2.8
BL-FI	2.7	0.9	0.6	0.7	2.7
BD-DI	80.0	87.0	23.0	12.6	1.2
CS-GG	5.3	9.0	3.1	2.8	0.7

TABLE 2

If one makes a Taylor Series expansion of the Jensity up to second order and integrates as in the DME, one arrives at a potential of the form

$$V_{\text{DME}}(r) = A \rho^2 + B \rho^3$$

where A and B are certain integrals over the two body potential (see eq. 4.11 in ²⁴). The leading term corresponds to a zero range force which would exactly reproduce the oscillations in ρ_n and in course of iterating would tend to amplify these oscillations in comparison to those of the original force. The second term tends to smooth out these oscillations because in general we have B less than zero and B^2 is positive at the relative maxima of ρ_n and negative for the minima. This argument is valid for nuclei with $N = Z$, for which the oscillations of ρ_n and ρ_p are in phase. It holds in particular for ^{138}Xe , even though N is somewhat larger than Z. For a heavy nucleus with an excess of neutrons ρ_n and ρ_p are no longer in phase. One must then take account of the fact that the field which dominates the proton distribution is determined to a great extent by ρ_n . The case of ^{208}Pb is very special because the oscillations of ρ_n and ρ_p are practically out of phase. The preceding argument can be applied but changing the sign of the correction term B^2 so that when there is a density maximum this term tends to increase further the oscillation.

In the DME calculations of Nogelo and Vautherin²⁴ it appears that the ρ^3 term overcorrects as one can see from their Fig. 3 where it appears that in the DME the density oscillations are attenuated in comparison to the exact calculation for ^{40}Ca , ^{48}Ca and ^{90}Zr , but are amplified for ^{138}Xe . For forces of the Skyrme type, where a term of the form ρ^3 appears in the HF field, the amplitude of the density fluctuations is closely tied to the strength of $(5t_1 - 9t_2)$. In the phenomenological adjustment the values of t_1 and t_2 are mainly determined by the surface energy, so that $(5t_1 - 9t_2)$ is probably not well defined. This could explain the large dispersion in the results for forces of this type.

Just as for the surface thickness the incompressibility and the density dependence play a role in determining the amplitude of the fluctuations. For a force with a high incompressibility any deviation from a uniform equilibrium density is resisted because it costs too much in energy. In practice, however, this effect can be seen only for very large and unphysical variations of K. Thus for example for the three forces of Sprung and Banerjee mentioned above one sees practically no influence on the oscillations (Fig. 11 of ref. 11).

The density dependence is more important. The force becomes more repulsive where the density increases, thus the force is more attractive where the density is small and less attractive where it is high. This tends to increase the number of particles in the minima and to reduce the number in the maxima, which certainly tends to smooth the oscillations. One observes such an effect for the Skyrme forces by increasing the value of t_1 , which makes the density distribution smoother.

From the comparison with experiment in Table 2 and Table 1 it is seen that for the heavy nuclei, where the present H.F. theory is more justified, the calculation based on a realistic effective interaction give better results than the purely phenomenological forces. This is for the reasons listed above. On the other hand for the lighter nuclei, the realistic force give too large density oscillations while for the same reasons the better agreement found for the Skyrme forces must be considered accidental. This is an unresolved problem.

A final remark concerns the average slope of the interior density that we characterize by the slope of the straight line defined at the beginning of this section. We have shown this slope for various calculations in Table 3 as well as its value for experimental charge densities. Using the same reasoning that in the cases of surface thickness and density fluctuations it is easy to see that the slope of the interior density is essentially governed by the incompressibility and by the strength of the density dependence of the interaction. From the comparison with experiment in Table 3 it is seen that forces with small K and weak density dependence yield unrealistic slopes.

FORCE	SLOPE OF THE INTERIOR DENSITY $10^{-3} \cdot \text{fm}^{-1}$				
	^{40}Ca	^{48}Ca	^{56}Ni	^{72}Kr	^{208}Pb
S-V;	-0.43	-0.26	-0.04	-0.15	0.01
S-III;	-0.55	-0.40	-0.04	-0.18	-0.92
S-V	-0.80	-0.65	-0.24	-0.38	-0.15
BL-F1	-0.72	-0.47	-0.29	-0.20	-0.13
BB-91	-1.51	-1.20	-0.57	-0.60	-0.48
CS-G3	-0.85	-0.57	-0.16	-0.38	-0.22
Exp.	-0.73	-0.44	-0.34	-0.03	-0.02

TABLE 3

4. Charge density differences between neighbouring nuclei

In this last section we will turn our attention to the question of differences in the charge densities between neighbouring nuclei. The mechanisms which govern these effects are different than those which we discussed earlier for the total charge density and therefore constitute an independent test of the theory.

In the framework of Hartree-Fock theory, the effects on the charge density can be interpreted more intuitively

using the concept of the polarizing field. This field is defined as the change in the equivalent local potential (ref.17,11) when particles are added to the nucleus. For an orbital $n_l r$ it is $V_{nl}(\Delta A) = V_{nl}(A+\Delta A) - V_{nl}(A)$ where the V_{nl} is the equivalent local field acting on a particle in the orbit $n_l r$. An examination of this field allows one to understand the changes in the densities—that is to say the regions towards which particles are preferentially attracted or from which they are repelled. As an example we show in Fig.3 the polarizing fields for neutrons and protons corresponding to the addition of 8 neutrons to the nucleus $^{114}\text{Sn}^{23}$. This calculation used the same interaction as in ref.11). It is clear that the effect on the neutrons is much weaker than on the protons, reflecting the fact that the neutron-proton interaction is much stronger than the neutron-neutron. The form of the polarizing field can be understood simply. In a self-consistent theory, the one-body potential follows the density. Having in mind something like a Fermi function depending on the variables $(r-R)/a$ we will have

$$\begin{aligned} \Delta V_F^{\text{pol}} &= \frac{1}{\rho_0} (V_0 + \Delta V_0) \rho \left(\frac{r-R-\Delta R}{a+\Delta a} \right) - \frac{V_0}{\rho_0} \rho \left(\frac{r-R}{a} \right) \\ &= \Delta V_0 \frac{1}{\rho_0} \rho \left(\frac{r-R}{a} \right) - V_0 \left[\Delta R + a \left(\frac{r-R}{a} \right) \frac{1}{\rho_0} \rho' \left(\frac{r-R}{a} \right) \right] \end{aligned} \quad (6)$$

Thus we expect ΔV^{pol} to contain both a volume contribution and a surface peaked contribution; the latter can be situated inside or outside the half density radius depending upon the sign of the change in diffusivity. Noting the importance of the unlike particle interaction we expect ΔV_0 to vanish for neutrons (when no protons are added) so the volume contribution will vanish. For protons there is a sizeable volume contribution which is evident in Fig.3. In the particular case of ^{114}Sn - ^{118}Sn we have found practically no change in diffusivity for the proton densities. This implies that $\Delta a = 0$ in formula (6). We see also in Fig.4 that the surface peaked term in ΔV_F^{pol} is very close to the half potential radius. Also shown in the figure is the equivalent local Hartree-Fock potential (for the $1g_{7/2}$ proton state) drawn on a reduced scale. By comparing with the change in neutron density in the same figure one sees a correspondence between $\Delta \rho_n$ and the polarizing field acting on the proton, which is consistent

With the approximation made in eq.(6).

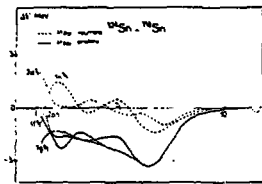


Fig. 3

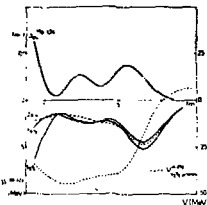


Fig. 4

Two other remarks should be made. First of all we see that $\Delta E_{\text{pol}}^{\text{pro}}$ for protons depends very little upon the state α . Both the very deep lying states and the states near the Fermi surface will be equally modified. It is therefore not sufficient to consider only the last few occupied shells of protons in calculations of the isotopes shift, as has been generally done in perturbative calculations. The second remark concerns the relation between the isotope shift and the compressibility of nuclear matter, used in the macroscopic models. First of all, because of surface, Coulomb and asymmetry effects, $K_{\text{inf}}^{\text{pro}}$ is greater than $K_{\text{inf}}^{\text{neut}}$. Moreover the neutrons and the protons behave completely differently when only one type of particle (protons) are pulled towards the surface by the added neutrons. As we have remarked in a different context²⁵⁾ the nucleus is much more rigid against compression (or dilatation) of the protons alone. Secondly, the polarizing field acting on the protons is not of the quadratic form one would use in calculating the compressibility of a finite nucleus.

Another point to be understood is the influence of the symmetry energy. As we have already said, the $\Delta E_{\text{pol}}^{\text{pro}}$ is essentially governed by the strength of the neutron-proton force.

Changing the symmetry energy alters the ratio of like to unlike particle forces, hence the field will change. However, we have observed that for changes in the symmetry energy, which remain roughly compatible with other properties of finite nuclei the effect on the magnitude of the isotope shift is rather weak. (We have considered changes in the symmetry energy in the ref.11). As these calculations were able to reproduce correctly other nuclear properties which are much more sensitive to symmetry energy (the single particle spectrum, the curvature of the mass parabola) we believe that the strength of the volume contribution is well determined by the theory.

A more detailed description of the polarizing field can be found in the thesis of J. Martorell²⁰⁾ which contains in particular an analytic form for the case of the Skyrme interaction. One finds there also other remarks on effects which play a role in the isotope shift. One of these concerns the influence of the spatial position of the orbit (and hence of its energy) in which the polarizing neutrons are placed. As we saw above the polarizing field is to first approximation proportional to the density of added neutrons. It will therefore depend on the position of the orbit they occupy. In a self-consistent calculation this position is completely determined but it must be admitted that the approximations usually introduced for treating the spin orbit interaction, the starting energy, and also the suppression of the tensor force, may modify the results to some degree. What is the sensitivity of the isotope shift calculation to these uncertainties? This effect was studied in the case of ^{40}Ca - ^{42}Ca simply by modifying the equivalent local potential for a $1f_{7/2}$ neutron by a constant multiplicative factor. Shifting the neutrons $1f_{7/2}$ energy by 4 MeV causes a change in the charge radius of ^{40}Ca by 0.006 fm (using the S-III Skyrme force). This is of the same order as the experimental difference between the charge radii of ^{40}Ca and ^{42}Ca . This could explain why certain calculations (see Fig.1), give a Δr much too large (and of the wrong sign) when the energy of the $1f_{7/2}$ state is not correct. This effect seems to be roughly independent of the number of protons so it should be less important for heavy nuclei. It is, however, critical for light nuclei. Another point concerns the single particle level density. A simple perturbation theory

argument explains this dependence qualitatively. The first order change in the wave function ψ_1 is given by

$$\delta \psi_1 = \sum_{n \neq 1} \frac{\langle \psi_n | \delta V | \psi_1 \rangle}{E_1 - E_n} \psi_n$$

So for the same δV^{pol} the changes in the wave functions will be greater when the levels are more closely spaced. This level density increases with the effective mass and as shown in ref.20) (for the particular case of a Skyrme interaction) δV^{pol} also increases with m^* . Hence the two effects work together to increase the isotope shift. This dependence was verified numerically with different Skyrme forces which give different m^* .

One could also ask to what extent does the self-consistency aspect of Hartree-Fock contribute to the results. In other words, what is the difference between a H.F. calculation and a second order perturbation theory calculation. This question which can only be studied numerically was looked at by Martorell²⁰⁾ particularly for the case of the isotope shift between ^{117}Sn - ^{118}Sn . In the first step, starting from the self-consistent solution for ^{117}Sn one carries out one additional iteration while adding 5 neutrons leading to a new charge density for the nucleus ^{117}Sn . In a second stage one obtains the completely self-consistent solution for ^{117}Sn . By comparing these two results one sees that the perturbative calculation gives the single particle energy well enough but the effects of polarization on the density are given only poorly. For example, for the proton radius one obtains only 80% of the self-consistent isotope shift. Similar results were obtained for other series of isotopes and isotonies. It seems therefore that for a quantitative detailed study one must make use of the completely self-consistent solutions.

4.1 Comparison with experimental results

To close this section we have selected a number of examples throughout the periodic table for which an adequate amount of electron and muonic data is available. The theoretical values were calculated by the method of (ref.11) but undoubtedly other density dependent forces would give similar results.

Calcium Isotopes

As was shown by Bertozzi, Friar, Heisenberg and Negele¹⁶⁾ the famous anomaly between the radii of ^{40}Ca - ^{48}Ca can be resolved by taking into account the neutron form factor and the electromagnetic spin orbit interaction. (See Fig.2). One must of course calculate the proton density correctly, using a force which reproduces the binding-energy difference between ^{40}Ca and ^{48}Ca and which places the $f_{7/2}$ neutron orbital correctly.

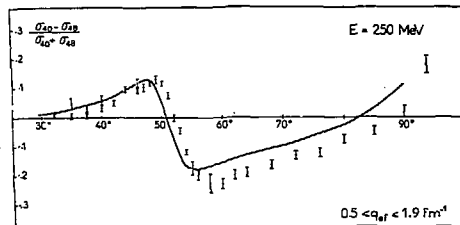


Fig.5

In Fig.5 we show the ratio of differential cross sections for electron scattering

$$\left[\frac{d\sigma}{d\Omega} (40) - \frac{d\sigma}{d\Omega} (48) \right] / \left[\frac{d\sigma}{d\Omega} (40) + \frac{d\sigma}{d\Omega} (48) \right]$$

Although the agreement with experiment can be considered good, it is nonetheless clear that some disagreement remains for the entire momentum transfers. Bertozzi et al.¹⁶⁾ attributed this presumably to a spurious isospin impurity introduced by H.F. in nuclei with $N \neq Z$. One could just as well attribute it to a shell closure effect, which is known to be more marked for ^{40}Ca than for ^{48}Ca . In this case the correction due to configuration mixing will be more important for ^{40}Ca than for ^{48}Ca , further reducing the radius anomaly.

... effects were included in a self-consistent manner in order to correctly take into account the partial occupation of the neutron orbitals. From what was said in the preceding section, the tin isotopes are a good place to examine the isotope shift. The validity of the charge density differences can be tested by comparison with the ratios of electron scattering cross sections. For the case of ^{112}Sn - ^{114}Sn we see in Fig. 6 a very good agreement up to $q \approx 1.4 \text{ fm}^{-1}$ with the experimental measurements of Fujimori et al.²⁶⁾ The change in charge radius between adjacent pairs of isotopes is plotted in Fig. 7. The triangles and dots

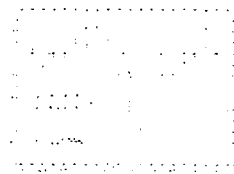


Fig. 6 - Ratio of differential cross sections for muonic scattering between ^{112}Sn and ^{114}Sn . The charge densities were calculated with H.F. densities; isotopic shifts are calculated with the phenomenological densities of ref. 26).

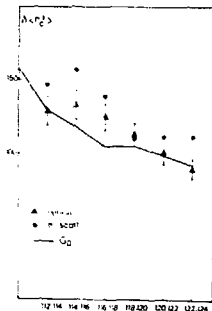


Fig. 7

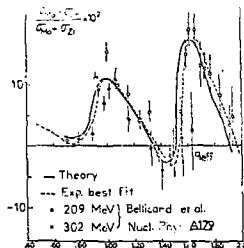


Fig. 8

present in the tin isotope shifts²³⁾.

Isotope shifts

The core polarization part of the isotope shift is relatively small because the proton-proton force is weaker than the neutron-proton force. Thus, adding protons has a small effect on the existing charge density and it is essentially the wave function of the added protons which describes directly the bulk of the effect. It seems difficult from the experimental data to determine the change in charge density in any very model independent way, so we will compare directly our calculated results with experimental data. Table 4 contains some typical results for muonic atom isotope shifts showing agreement comparable to that found for isotope shifts above. Electron scattering cross section ratios for $^{112}\text{Sn}/^{114}\text{Sn}$ are shown in Fig. 8 while those for Bi/Pb are in Fig. 9. The latter

are μPb^{208} and elastic electron scattering respectively. The latter have no assigned error but it would be large. Here the neutron and spin orbital contributions are important in improving the slope of the $\delta(\rho)$ curve. We find moreover that the neutron contribution reduces the diffusivity of the charge density more for the heavy isotopes than for the light, which could explain the experimentally observed reduction in diffusivity²⁶⁾. We can conclude that this contribution is indeed

	$2p_{3/2} - 1s_{1/2}$		$2p_{1/2} - 1s_{1/2}$	
	Th	Exp	Th	Exp
$^{40}\text{Ca} - ^{41}\text{K}$	71.14	70.92 ± 0.15 (K_{α})	70.87	70.92 ± 0.15 (K_{α})
$^{88}\text{Sr} - ^{89}\text{Sr}$	195.4	191.3 ± 1.6 (K_{α})	191.9	193.3 ± 1.6 (K_{α})
$^{90}\text{Zr} - ^{91}\text{Zr}$	195.7	196.4 ± 1.2	191.5	191.9 ± 1.2
$^{114}\text{Sn} - ^{115}\text{Cd}$	200.2	201.0 ± 0.3	194.1	195.4 ± 0.3
$^{124}\text{Te} - ^{125}\text{Sn}$	184.0	185.0 ± 0.3	177.7	178.6 ± 0.4
$^{208}\text{Pb} - ^{209}\text{Tl}$	66.6	65.5 ± 1.4	61.5	60.7 ± 1.3
$^{210}\text{Bi} - ^{210}\text{Po}$	69.7	71.2 ± 2.9	64.1	65.3 ± 3.1

TABLE 4

is practically identical to the results found by Sick, Flocard and Vénéroni²⁸⁾, using the Skyrme-II force. Here the effect of polarization is quite important whereas for the case of Mo/Zr we find that the change in charge density is given almost completely by the wave function of the protons in the $1g_{7/2}$ state. This difference between the two cases can be understood following the considerations in Section 4.1 on the position of the polarizing orbital and on the level density.

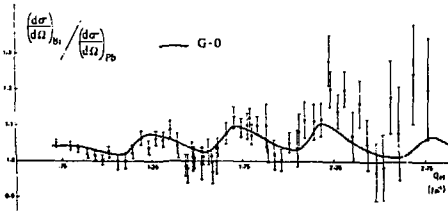


Fig. 9

Acknowledgements

The author is very indebted to D.W.L. Sprung for help in the preparation of this review and to I. Sick and J.B. Belliard for making experimental data on ^{88}Ni available prior to publication.

References

- 1) J. Friar and J.W. Negele, Nucl. Phys. A 212 (1973) 93
- 2) I. Sick, Phys. Lett. 44B (1973) 62; Nucl. Phys. A 218 (1974) 509
- 3) I. Sick, Phys. Lett. 53B (1974) 15
- 4) D.W.L. Sprung, Private communication
- 5) L.A. Fajardo, J.R. Flocard, W.P. Trower, I. Sick, Phys. Lett. 37B (1971) 363
- 6) R. Engler et al., Nucl. Data, to be published
- 7) I. Sick, J.B. Belliard, M. Bernholm, A. Bussière de Nercy, B. Frois, M. Huert, Ph. Leconte, J. Mougey, Pham Xuan Ho, D. Royer and S. Turck, to be published
- 8) J. Friar and J.W. Negele, Adv. Nucl. Phys., ed. M. Banerjee and E. Vogt, to be published (1975)
- 9) D.W.L. Sprung and P.K. Banerjee, Nucl. Phys. A168 (1971) 273
- 10) M. Beiner, H. Flocard, Nguyen Van Giai and Ph. Quentien, Nucl. Phys. A238 (1975) 29
- 11) X. Campi and D.W.L. Sprung, Nucl. Phys. A 194 (1972) 401
- 12) J.V. Ehlers, S.A. Moszkowski, Phys. Rev. C6 (1972) 217
- 13) M. Beiner, E. Lombard, Ann. of Phys. 86 (1974) 262
- 14) G. Fai and J. Womath, Nucl. Phys. A 208 (1973) 463
- 15) S.A. Coon and H.S. Kähler, Nucl. Phys. A 231 (1974) 75
- 16) W. Bertozzi, J. Friar, J. Helsenberg and J.W. Negele, Phys. Lett. 41B (1972) 408
- 17) D. Vautherin and M. Vénéroni, Phys. Lett. 25B (1967) 175
- 18) J.W. Negele, Phys. Rev. C9 (1974) 1054
- 19) E.M. Steink and E. Bonker, Nucl. Phys. A91 (1967) 1
- 20) J. Martorell, Thesis, Universidad Autonoma de Madrid, Spain (1974)
- 21) K. Lessey, Nucl. Phys. A192 (1972) 177
- 22) A. Faessler, J.E. Galonska, K. Gozke and S.A. Moszkowski, Nucl. Phys. A, to be published
- 23) X. Campi, D.W.L. Sprung and J. Martorell, Nucl. Phys. A 223 (1974) 541
- 24) J.W. Negele, D. Vautherin, Phys. Rev. C5 (1972) 1472
- 25) J. Martorell and X. Campi, Phys. Lett. 46B (1973) 296
- 26) L.A. Fajardo, J.R. Flocard, W.P. Trower and I. Sick, Phys. Lett. 42B (1972) 213
- 27) R.C. Barrett, Reports on progress in physics (1973)
- 28) I. Sick, H. Flocard and M. Vénéroni, Phys. Lett. 39B (1972) 443
- 29) J.W. Negele, Phys. Rev. Cl (1970) 1260